Lattice vibrations in $Rb_{1-c}K_c$ alloys: Shortcomings of a single-site coherent potential approximation*

Mark Mostoller and Theodore Kaplan
Solid State Division, Oak Ridge National Laboratory, Oak Ridge, Tennessee 37830
(Received 2 May 1977)

A single-site coherent potential approximation (CPA) including force constant changes in the additive limit (designated the CPA-F) is applied to phonons in $Rb_{1-c}K_c$ alloys. The CPA-F results are in better overall agreement with the neutron scattering measurements of Kamitakahara and Copley than mass-defect CPA results. However, marked discrepancies in the concentration, branch, and wave-vector dependence and in the line shapes remain between CPA-F and experimental neutron scattering cross sections. These discrepancies suggest the need to include multiple scattering from pairs and larger clusters in the theoretical treatment.

I. INTRODUCTION

Lattice vibrations in alloys provide a particularly severe testing arena for any theory of elementary excitations in disordered systems because the frequency–wave-vector relationship for phonons can be measured directly by coherent inelastic neutron scattering. Furthermore, the one-phonon incoherent neutron scattering cross section gives information about a suitably weighted phonon density of states. In the early 1960's, a number of experimental groups began to apply neutron scattering to the study of lattice vibrations in alloys. Early incoherent scattering experiments on Pd-Ni alloys and on vanadium-based alloys were performed at Brookhaven.[1,2] Coherent neutron scattering measurements were done on Cu-Au alloys at Chalk River,[3] on Cr-W at Risø,[4] and on the Cu-Al system at Oak Ridge.[5]

These early experiments showed that phonons in alloys behaved qualitatively as expected. When lighter mass impurities were alloyed into a host lattice of heavier atoms, local mode peaks were observed above the maximum phonon frequency of the host.[1,2,5] The introduction of heavier mass impurities produced resonant mode effects within the frequency spectrum of the host crystal.[2-4] Not surprisingly, however, the experimental results did not generally agree with the predictions of a low concentration theory for mass defects only.[6] In this theory, the phonon self-energy produced by isotopic impurities was approximated by the product of the impurity concentration and the scattering or t matrix for a single impurity (symbolically, $E = ct$, where E is the self-energy, c is the concentration, and t is the scattering matrix for a single defect). The principal features of this model are (i) neither volume-dependent nor local force constant changes are included; (ii) the theory is correct to first order in the defect concentration; (iii) in the alloy, the in-band modes, that is, phonons with frequencies within the spectrum of the host crystal, are shifted and broadened by an amount which depends only on the phonon frequency, and not on the wave vector; (iv) when lighter mass impurities give rise to local modes, these modes are δ functions with no intrinsic width.

The work of Bruno and Taylor[7] and of Kesharwani and Agrawal[8,9] showed that substantially better, but not complete, agreement with experiment could be obtained for[7,8] dilute $Cu_{1-c}Au_c$ and[9] $Cr_{1-c}W_c$ alloys if two kinds of force constant changes were incorporated in the theoretical model. First, the host-crystal force constants were modified to approximate the effects of the volume expansion of the lattice on alloying. Second, local force constant changes around the impurity atoms were treated, along with the mass differences, in the $E = ct$ approximation[10] or in the slightly more sophisticated approach of Elliott and Taylor.[11] The phonon frequencies in the alloy are shifted with respect to those of the pure host by the overall modification of the force constants. The in-band modes are further shifted and broadened by the local mass and force constant changes, and these shifts and widths now depend on the phonon wave vector as well as its frequency.

The approach of Bruno and Taylor and of Kesharwani and Agrawal is correct only to first order in the defect concentration, and if local modes are predicted, they have no intrinsic width. For their purposes, however, these features of their treatment were relatively unimportant, since they were dealing with rather low concentrations of heavy mass impurities.

To span the whole concentration range for phonons in alloys with mass disorder only, Taylor[12] introduced the so-called coherent potential approximation (CPA); the same approximation for the electronic states of alloys was proposed simultan-

eously by Soven.[13] In the CPA for mass defects, an effective crystal is constructed which has a complex, frequency-dependent and site-diagonal self-energy; this self-energy is determined self-consistently such that the average scattering from a single real atom in the effective crystal vanishes. Taylor showed that the mass-defect CPA gave results for the density of states which were in good overall agreement with "exact" machine calculations[14,15] for isotopically disordered one- and three-dimensional alloys. However, the CPA failed to reproduce structure in the density of states arising from pairs and larger clusters. A major qualitative difference between the CPA and alternative, non-self-consistent theories[11,16] is that in the CPA, local mode peaks above the host band are no longer δ functions, but are broadened by the imaginary part of the self-energy.

The mass-defect CPA has been applied to a number of alloys which have been studied by neutron scattering. These include Cu-Au,[12] Ni-Pt,[17] Ge-Si,[18] Cu-Al and $(K\text{-}NH_4)Cl$,[19] Rb-K,[20] Ni-Pd,[21] Y-Tb,[22] and Mo-Re.[23] Except possibly for the Ge-Si and Y-Tb systems, the mass-defect CPA results were not in quantitative agreement with the experimental data. Discrepancies between calculated and observed peak positions and/or shapes indicated the need for a theory which included force constant changes as well as mass disorder. Furthermore, it seemed likely that cluster (rather than just single-site) scattering effects might have to be incorporated, although there was no unambiguous experimental evidence of such effects.

Several extensions of the CPA to include off-diagonal as well as diagonal disorder have been proposed.[24-30] We shall focus on one of these, which was recently described by the present authors,[27] Niizeki,[28] and Fukuyama *et al.*,[29] but which was originally put forward by Takeno[30] in a paper that has been largely overlooked. The basic assumption of this approach, which we will call the CPA-F, is that the force constants (for electrons, the transfer or hopping integrals) in the alloy superimpose linearly. This assumption is sometimes referred to as the additive limit, because for a monatomic A-A' alloy, the requirement is that the A-A' force constants be the arithmetic average of the A-A and A'-A' force constants.

Given the assumption of linear superposition, each defect carries with it a perturbation which can be identified with the defect site but which has finite range. As in the mass-defect CPA, an effective crystal is constructed, with a complex, frequency-dependent, but now spatially extended, self-energy matrix; the spatial range of the self-energy matrix is determined by that of the defect perturbations. The self-energy is then found self-consistently by requiring that the scattering from the extended perturbations of single defect or host atoms in the effective crystal vanish on the average.

The authors have shown that CPA-F results for the density of states of one-dimensional alloys with off-diagonal as well as diagonal disorder exhibit the same kind of overall agreement with exact calculations as does the mass-defect CPA for isotopically disordered linear chains.[27] We have also applied the CPA-F to $K_{1-c}(NH_4)_cCl$,[31] and obtained better agreement with neutron scattering data[32] than could be achieved with the mass-defect CPA.[19] Niizeki[28] and Fukuyama *et al.*[29] have shown that the CPA-F is equivalent to the treatment of Blackman *et al.*[25] for an electronic tight-binding Hamiltonian which satisfies the condition of linear superposition. Alben *et al.*[33] have compared CPA-F results with those of large cluster calculations for s electrons in binary simple cubic alloys. They found that the CPA-F and "exact" results agreed relatively well not only for the density of states, but also for the spectral function $A(\vec{k}, E)$ which corresponds to the coherent neutron scattering cross section for phonons.

In this paper, we apply the CPA-F with nearest-neighbor radial force constant changes to the phonon spectra of $Rb_{1-c}K_c$ alloys.[34] Kamitakahara and Copley[20] have performed coherent neutron scattering measurements on this system at three concentrations, $c = 0.06$, 0.18, and 0.29. Data were taken for the longitudinal mode propagating along the [110] direction at all three concentrations, and for the transverse mode along the [001] direction at $c = 0.18$ and 0.29. The neutron groups exhibited local mode peaks corresponding to the motion of the light potassium atoms in the heavier rubidium host lattice, and these grew in intensity as the potassium concentration increased. The in-band peaks also shifted by small amounts with respect to the phonon frequencies in pure Rb.

Mass-defect CPA calculations for $Rb_{1-c}K_c$ gave results which did not agree with experiment. The calculated in-band and local mode peak positions were generally too low and too high, respectively, but the most striking discrepancies occurred in the line shapes for scattering wave vectors near the Brillouin zone boundaries: the two-peaked structure of the neutron groups for these wave vectors was much sharper than that predicted by the mass-defect CPA. While it appeared possible that including force constant changes within the CPA would give better agreement for the peak positions, it seemed unlikely that line shapes matching experiment would be obtained. As will be shown, our CPA-F results confirm these expectations. Furthermore, no CPA-F treatment with nearest-

neighbor radial force constant changes only can reproduce the observed branch and concentration dependence of the neutron scattering. While perhaps not conclusive, the evidence is strong that a theoretical treatment which goes beyond the single-site approach of the CPA is needed to explain the data for Rb-K alloys.

The paper is organized as follows. Section II provides a brief description of the CPA-F theory, and shows how to calculate the coherent neutron scattering cross section within the framework of the the model. CPA-F and mass defect CPA results for $Rb_{1-c}K_c$ are presented and compared with experiment in Sec. III. Conclusions are discussed in Sec. IV.

II. THEORY

One-phonon Green's functions are defined in the usual way[12,27] as the time transforms of retarded displacement-displacement correlation functions. The perfect host crystal Green's function $\underline{P}(l,l';\omega)$ satisfies the equation

$$\underline{I}\,\delta(l,l') = \sum_{l''} \{M\omega^2 \underline{I}\,\delta(l,l'') - \underline{\Phi}^0(l,l'')\} \cdot \underline{P}(l'',l';\omega), \tag{1}$$

where $\underline{I}$ is the unit matrix, M is the host atomic mass, ω is the frequency, and $\underline{\Phi}^0(l,l') = \underline{\Phi}^0(l-l')$ is the force constant matrix coupling atoms at sites l and l'. The host or reference crystal need not represent either pure constituent; in particular, volume-dependent force constant changes may be incorporated in the matrices $\underline{\Phi}^0(l,l')$.

With the assumption that the force constants in the alloy superimpose linearly, the equation for the Green's function $\underline{G}(l,l';\omega)$ in the presence of defects can be written in the form

$$\underline{I}\,\delta(l,l') = \sum_{l''} \Big\{ M\omega^2 \underline{I}\,\delta(l,l'') - \underline{\Phi}^0(l,l'') - \sum_{l_i} \underline{\mathfrak{D}}^{\gamma(l_i)}(l,l'';\omega) \Big\} \cdot \underline{G}(l'',l';\omega), \tag{2}$$

in which $\underline{\mathfrak{D}}^{\gamma(l_i)}$ is the perturbation produced by an atom of type γ at the site l_i. If a host atom is at l_i, i.e., $\gamma(l_i) = h$, then the perturbation is zero,

$$\underline{\mathfrak{D}}^{h(l_i)}(l,l';\omega) = 0. \tag{3}$$

If a defect is at l_i, the perturbation will be nonzero over a range of sites s,s' around l_i which will be called the defect space,

$$\underline{\mathfrak{D}}^{d(l_i)}(l,l';\omega) = \sum_{ss'} \underline{D}(s,s';\omega) \times \delta(l,s+l_i)\delta(l',s'+l_i). \tag{4}$$

Here $\underline{D}(s,s';\omega) = \underline{\mathfrak{D}}^{d(0)}(s,s';\omega)$ includes both mass and force constant changes,

$$\underline{D}(s,s';\omega) = M\epsilon\omega^2 \underline{I}\,\delta(s,0)\delta(s',0) + \Delta\underline{\Phi}(s,s'), \tag{5}$$

$$\epsilon = (M - M')/M, \tag{6}$$

where M' is the defect mass, and the $\Delta\underline{\Phi}(s,s')$ are the local force constant changes around a defect at site 0.

The model we will use for $Rb_{1-c}K_c$ is one in which there are nearest-neighbor force constant changes only. For this case, let n label one of the first neighbors of site 0. In order to satisfy the assumption of linear superposition, the $0-n$ defect-host force constants must be the arithmetic average of the defect-defect and host-host force constants,

$$\underline{\Phi}^{dh}(0,n) = \tfrac{1}{2}\{\underline{\Phi}^{dd}(0,n) + \underline{\Phi}^{hh}(0,n)\}. \tag{7}$$

For phonons, translational invariance requires that changes in the off-diagonal coupling constants be accompanied by changes in the site-diagonal or self terms. Hence the local force constant changes corresponding to Eq. (7) are

$$\Delta\underline{\Phi}(0,n) = \underline{\Phi}^{dh}(0,n) - \underline{\Phi}^0(0,n) = \tfrac{1}{2}\{\underline{\Phi}^{dd}(0,n) - \underline{\Phi}^{hh}(0,n)\}, \tag{8a}$$

$$\Delta\underline{\Phi}(n,n) = -\Delta\underline{\Phi}(0,n), \tag{8b}$$

$$\Delta\underline{\Phi}(0,0) = -\sum_n \Delta\underline{\Phi}(0,n). \tag{8c}$$

In the coherent potential approximation, a periodic effective medium is defined. The propagation of phonons in this effective medium is described by the CPA-F Green's function $\underline{G}^0(l,l';\omega)$, which satisfies

$$\underline{I}\,\delta(l,l') = \sum_{l''} \{M\omega^2 \underline{I}\,\delta(l,l'') - \underline{\Phi}^0(l,l'') - \underline{E}(l,l'';\omega)\} \cdot \underline{G}^0(l'',l';\omega), \tag{9}$$

where $\underline{E}(l,l';\omega) = \underline{E}(l-l';\omega)$ is a complex self-energy matrix. To develop an extended single-site approximation for the alloy, the translationally invariant self-energy $\underline{E}$ is decomposed into an overlapping set of local self-energy matrices $\underline{K}$ around every site in the crystal,

$$\underline{E}(l,l';\omega) = \sum_{l_i} \sum_{ss'} \underline{K}(s,s';\omega) \times \delta(l,s+l_i)\delta(l',s'+l_i). \tag{10}$$

In the CPA-F crystal, the local perturbations produced by host and defect atoms are $-\underline{K}$ and $\underline{D}-\underline{K}$, respectively.

As shown in Ref. 27, it is straightforward to follow in the steps of Taylor's derivation of the mass-defect CPA, but now with spatially extended local perturbations. The Green's function for the

alloy is $\langle \underline{G} \rangle$, where $\langle\ \rangle$ denotes configurational averaging. $\langle \underline{G} \rangle$ is expressed as a series involving $\underline{G}^0$ and the t matrices for scattering from host and defect atoms in the CPA-F crystal. The self-energy is chosen so that, on the average, the single-site scattering vanishes; symbolically, $0 = (1-c)\underline{T}^h + c\underline{T}^d$. The resulting equation for the local self-energy is

$$0 = \underline{K}(s,s';\omega) - c\underline{D}(s,s';\omega) + \sum_{s_1 s_2} \underline{K}(s,s_1;\omega) \cdot \underline{G}^0(s_1,s_2;\omega) \cdot [\underline{K}(s_2,s';\omega) - \underline{D}(s_2,s';\omega)]. \quad (11)$$

Equations (9)–(11) comprise a closed set of complex matrix equations for $\underline{G}^0$, $\underline{E}$, and $\underline{K}$ which must be solved self-consistently.

To determine the neutron scattering cross section within the CPA-F, it is necessary to evaluate conditionally averaged Green's functions, in which it is known, for example, that a host atom is at site l and a defect is at l'. In Ref. 31, the authors showed how to find the CPA-F density of states and the incoherent scattering cross section, but asserted that it was not feasible to calculate the coherent cross section exactly within the confines of the model. Niizeki[28] has since shown that it is possible to determine the CPA-F coherent cross section. The procedure for doing so is outlined in the Appendix.

Thermal-average scattering lengths for host and defect atoms, including the appropriate Debye-Waller factors,[28] are denoted by $\langle A_h \rangle_{\rm th}$ and $\langle A_d \rangle_{\rm th}$, respectively. In this notation, the incoherent atomic cross sections are proportional to $\langle (\Delta A_\gamma)^2 \rangle_{\rm th}$,

$$\langle (\Delta A_\gamma)^2 \rangle_{\rm th} = \langle A_\gamma^2 \rangle_{\rm th} - \langle A_\gamma \rangle_{\rm th}^2. \quad (12)$$

As is evident from Eq. (A14), the matrix ratio $\underline{D}^{-1} \cdot \underline{K}$ of the local self-energy to the perturbation must appear in the final expression for the scattering cross section. We define

$$\underline{F}(s,s';\omega) = \sum_{s_1} \underline{D}^{-1}(s,s_1) \cdot \underline{K}(s_1,s'), \quad (13)$$

$$\underline{F}(\vec{q};\omega) = \sum_s e^{-i\vec{q}\cdot\vec{R}(s)} \underline{F}(0,s;\omega), \quad (14)$$

where $\vec{R}(s)$ is the lattice vector from site 0 to site s.

We are now prepared to write the CPA-F expression for the one-phonon neutron scattering structure factor

$$\langle S(\vec{Q},\omega) \rangle = \langle S_{\rm incoh}(\vec{Q},\omega) \rangle + \langle S_{\rm coh}(\vec{Q},\omega) \rangle\ , \quad (15)$$

which describes the scattering of a neutron through a wave vector $\vec{Q}$ with an energy transfer $\hbar\omega$ to the lattice. The incoherent and coherent structure factors are, respectively,

$$\langle S_{\rm incoh}(\vec{Q},\omega) \rangle = \vec{Q} \cdot {\rm Im} \Big\{ \langle (\Delta A_h)^2 \rangle_{\rm th} \underline{G}^0(0,0;\omega) + [\langle (\Delta A_d)^2 \rangle_{\rm th} - \langle (\Delta A_h)^2 \rangle_{\rm th}] \sum_s \underline{F}(0,s;\omega) \cdot \underline{G}^0(s,0;\omega) + [\langle A_d \rangle_{\rm th} - \langle A_h \rangle_{\rm th}]^2 \Big[\sum_s \underline{F}(0,s;\omega) \cdot \underline{D}^{-1}(s,0) - c\underline{D}^{-1}(0,0) \Big] \Big\} \cdot \vec{Q}, \quad (16)$$

$$\langle S_{\rm coh}(\vec{Q},\omega) \rangle = \vec{Q} \cdot {\rm Im} \{ [\langle A_h \rangle_{\rm th} \underline{I} + (\langle A_d \rangle_{\rm th} - \langle A_h \rangle_{\rm th}) \underline{F}(\vec{Q},\omega)] \cdot \underline{G}^0(\vec{Q},\omega) \cdot [\langle A_h \rangle_{\rm th} \underline{I} + (\langle A_d \rangle_{\rm th} - \langle A_h \rangle_{\rm th}) \underline{F}^\dagger(\vec{Q},\omega)] \} \cdot \vec{Q}. \quad (17)$$

For comparison, the approximation used by the authors in Ref. 31 was

$$\langle S_{\rm coh}(\vec{Q},\omega) \rangle \cong (\langle A \rangle_{\rm th})_{\rm av}^2 \vec{Q} \cdot {\rm Im} \underline{G}^0(\vec{Q},\omega) \cdot \vec{Q}, \quad (18)$$

$$(\langle A \rangle_{\rm th})_{\rm av} = (1-c)\langle A_h \rangle_{\rm th} + c\langle A_d \rangle_{\rm th}. \quad (19)$$

For our CPA-F calculations on $Rb_{1-c}K_c$ alloys, we will assume that only the nearest-neighbor radial force constants change locally. These are by far the largest force constants in the pure materials,[35-37] more than a factor of 5 greater than the radial second-neighbor interactions, and about 20 times larger than the tangential first-neighbor force constants. The local perturbation matrices $\underline{D}$ for bcc crystals are then written as

$$\underline{D}(000,111) = -\underline{D}(111,111) = -\tfrac{1}{3}\Delta \begin{pmatrix} 1 & 1 & 1 \\ 1 & 1 & 1 \\ 1 & 1 & 1 \end{pmatrix}, \quad (20)$$

$$\underline{D}(000,000) = (M\epsilon\omega^2 + \tfrac{8}{3}\Delta)\underline{I}, \quad (21)$$

where Δ is the nearest-neighbor radial force constant change.

Counting a central atom and its eight first neighbors, each with three Cartesian displacements, Eq. (11) for the local self-energy is a 27×27 matrix equation. This can be block diagonalized[10,31] into a T_{1u} 2×2 and A_{1g}, T_{2g}, and A_{2u} 1×1 equations. The various irreducible representations contribute differently to different phonon modes. For example, the T_{1u}, A_{1g}, and T_{2g} local self-energies contribute for longitudinal modes propaga-

ting along the $[\zeta,\zeta,0]$ direction in reciprocal space, and the T_{1u} and T_{2g} for the $[0,0,\zeta]$ transverse modes. At the zone boundaries for both, i.e., for the longitudinal mode at $\vec{Q}=(2\pi/a)(\frac{1}{2},\frac{1}{2},0)$ and the transverse mode at $\vec{Q}=(2\pi/a)(0,0,1)$, a single combination of the T_{1u} local self-energy elements contributes.

Although considerable simplification is gained by the point symmetry reduction of the problem, there remain six complex equations which must be solved self-consistently, and the real space CPA-F Green's functions in these equations must be evaluated by summation over the Brillouin zone. For the calculations reported in the next section, we summed over 728 points on a regular mesh in the irreducible $\frac{1}{48}$th of the zone. It was not necessary to add an imaginary part to the frequency in these summations, or to sum over more points in particular regions of the zone, because the imaginary parts of the CPA-F self-energies were sufficiently large in the frequency range of interest. Roughly 30 min on an IBM 360-91 computer were required to calculate the self-energies and the neutron scattering cross sections for a given defect concentration c and force constant change Δ.

Although the calculations are tractable, they are rather elaborate in view of the simplicity of the theoretical model: only single-site scattering is included; the force constants are assumed to superimpose linearly; only changes in the radial nearest-neighbor force constants are allowed; the crystal structure is a cubic Bravais lattice. If more local force constant changes were included, or if a crystal lattice of lower symmetry were involved, the calculations would become still more elaborate and time consuming.

III. RESULTS

For the host crystal in both our CPA-F and mass defect CPA calculations, we use the Rb mass and virtual crystal force constants, that is, concentration weighted averages of the (low-T) force constants for pure Rb,[36] and pure K,[37]

$$\underline{\Phi}^{0}(l,l')=(1-c)\underline{\Phi}^{\mathrm{Rb}}(l,l')+c\underline{\Phi}^{\mathrm{K}}(l,l'). \tag{22}$$

This is a convenient way in which to try to approximate the effects of the volume contraction of the lattice on alloying. As will be noted, CPA-F calculations were also done with two other sets of host force constants, but the virtual host results appeared to be superior for the in-band modes. The phonon frequencies in the virtual host crystal are slightly higher than they are in pure Rb. The mass defect introduced by a potassium atom is $\epsilon=[M(\mathrm{Rb})-M(\mathrm{K})]/M(\mathrm{Rb})=0.54$, and the radial nearest-neighbor force constant change Δ is treated as an adjustable parameter which is independent of the concentration. The values used for the various atomic scattering factors are $\langle A_{\mathrm{Rb}}\rangle_{\mathrm{th}}=0.708$, $\langle A_{\mathrm{K}}\rangle_{\mathrm{th}}=0.370$, $\langle(\Delta A_{\mathrm{Rb}})^2\rangle_{\mathrm{th}}=0.0$, and $\langle(\Delta A_{\mathrm{K}})^2\rangle_{\mathrm{th}}=0.0382$.

Figure 1 illustrates the difference between the CPA-F coherent cross section as calculated from Eq. (17) and the average scattering length approximation of Eqs. (18) and (19). The curves shown are for $c=0.18$, $\Delta=-300$ dyn/cm, and $\vec{Q}=(2\pi/a)(2.45,2.45,0)$, and as in all of our calculated "constant Q" scans, a Gaussian instrumental resolution function has been folded into the results. In the average scattering length approximation, the local mode peak is much stronger relative to the lower frequency in-band peak; in effect, this approximation overestimates the contributions made by the vibrations of the lighter potassium atoms and underestimates those of the rubidium atoms. This occurs because of the large difference in scattering lengths, $\langle A_{\mathrm{Rb}}\rangle_{\mathrm{th}}=1.9\langle A_{\mathrm{K}}\rangle_{\mathrm{th}}$. For results given subsequently, the full CPA-F expressions (16) and (17) are used to calculate the cross section.

Figure 2 shows the calculated cross section for $\vec{Q}=(2\pi/a)(2.5,2.5,0)$, $c=0.18$, and several values of Δ. In the mass defect CPA, i.e., for $\Delta=0$, the in-band peak frequency is 1.47 THz and the local mode frequency is 1.93 THz. For $\Delta=-300$ dyn/cm, which corresponds to a reduction of 13% in the nearest-neighbor radial force constant, the in-band peak moves upward slightly to 1.49 THz, while the

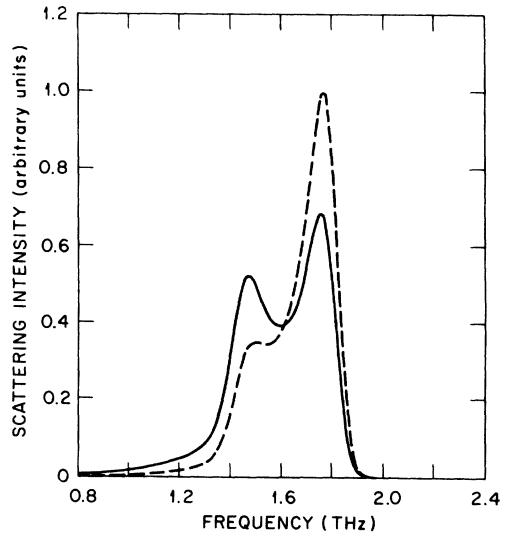

FIG. 1. Exact and approximate CPA-F coherent scattering cross sections for $c=0.18$ at $\vec{Q}=(2\pi/a)(2.45, 2.45, 0)$, including resolution (FWHM = 0.10 THz). The full curve gives the exact CPA-F cross section calculated from Eq. (17), and the dashed curve the average scattering length approximation results calculated from Eqs. (18) and (19).

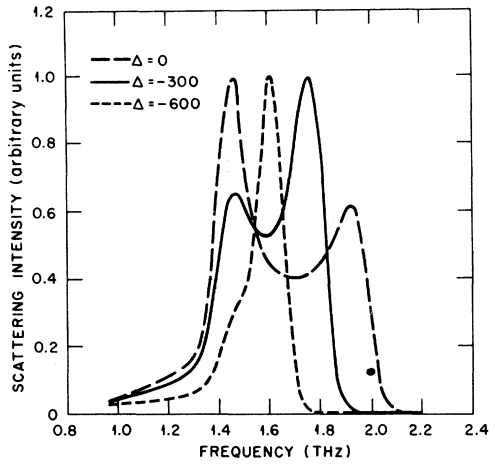

FIG. 2. CPA-F cross sections, including resolution (FWHM = 0.10 THz), for $c = 0.18$ and $\vec{Q} = (2\pi/a)(2.5, 2.5, 0)$ at several values of Δ.

local mode shifts down to 1.76 THz. Doubling Δ to −600 dyn/cm brings the local mode down still further so that a single peak at 1.62 THz occurs, with a modest shoulder on the low-frequency side.

Figure 3 illustrates the behavior of the cross section as a function of concentration for $\Delta = -300$ and $\vec{Q} = (2\pi/a)(2.5, 2.5, 0)$. As the potassium concentration increases, the local mode peak becomes more intense and moves to higher frequencies, while the in-band peak loses intensity but shifts little in frequency.

Experimental, CPA-F (Δ = −300), and mass-defect CPA results for the shifts in the in-band peak positions are compared in Fig. 4; the shifts are relative to the pure Rb frequencies calculated from

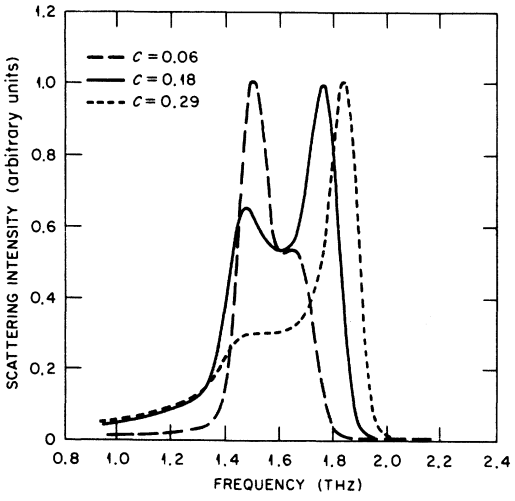

FIG. 3. Calculated cross sections, including resolution (FWHM = 0.10 THz), for Δ = −300, $\vec{Q} = (2\pi/a)(2.5, 2.5, 0)$, and $c = 0.06$, 0.18, and 0.29.

the 12K Born–von Kármán model of Copley and Brockhouse.[36] The CPA-F and mass-defect CPA peak positions were obtained directly from calculated curves for the neutron scattering cross section, with resolution folded in. Uncertainties in the experimental values were estimated by visual inspection of the neutron groups. For the in-band frequency shifts, the CPA-F with Δ = −300 appears to be in generally better agreement with experiment than the mass defect CPA. CPA-F and mass-defect CPA calculations were also performed using pure Rb rather than virtual crystal force constants for the host lattice, and the results for the in-band peak shifts were not as good as those shown in Fig. 4; the calculated in-band peaks were generally too low in frequency.

Figure 5 compares calculated scattering cross section curves with the observed neutron groups for two zone-boundary modes at several concentrations. Experimental error bars were determined as the square root of the number of counts, and linear backgrounds were subtracted from the raw experimental data prior to renormalization to maximum intensities of 1. Resolution is included in the calculated results.

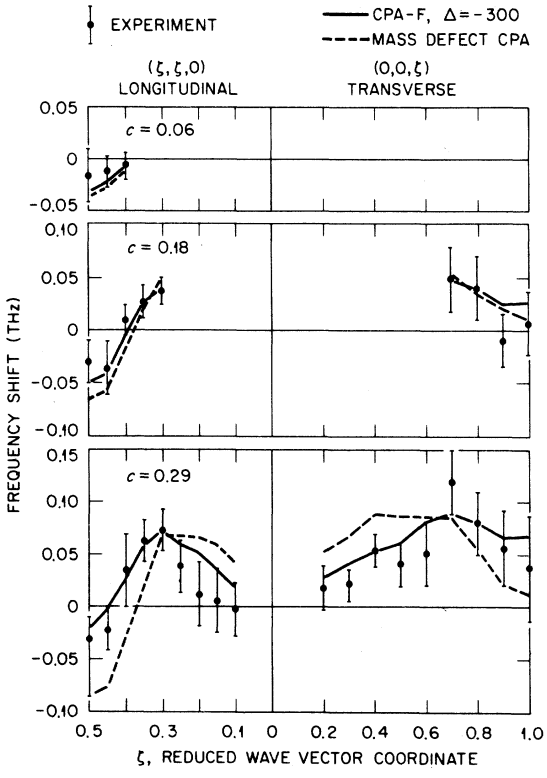

FIG. 4. CPA-F (Δ = −300), mass-defect CPA, and experimental results for the in-band mode peak shifts of $Rb_{1-c}K_c$ alloys relative to the 12K Born–von Kármán frequencies of pure Rb.

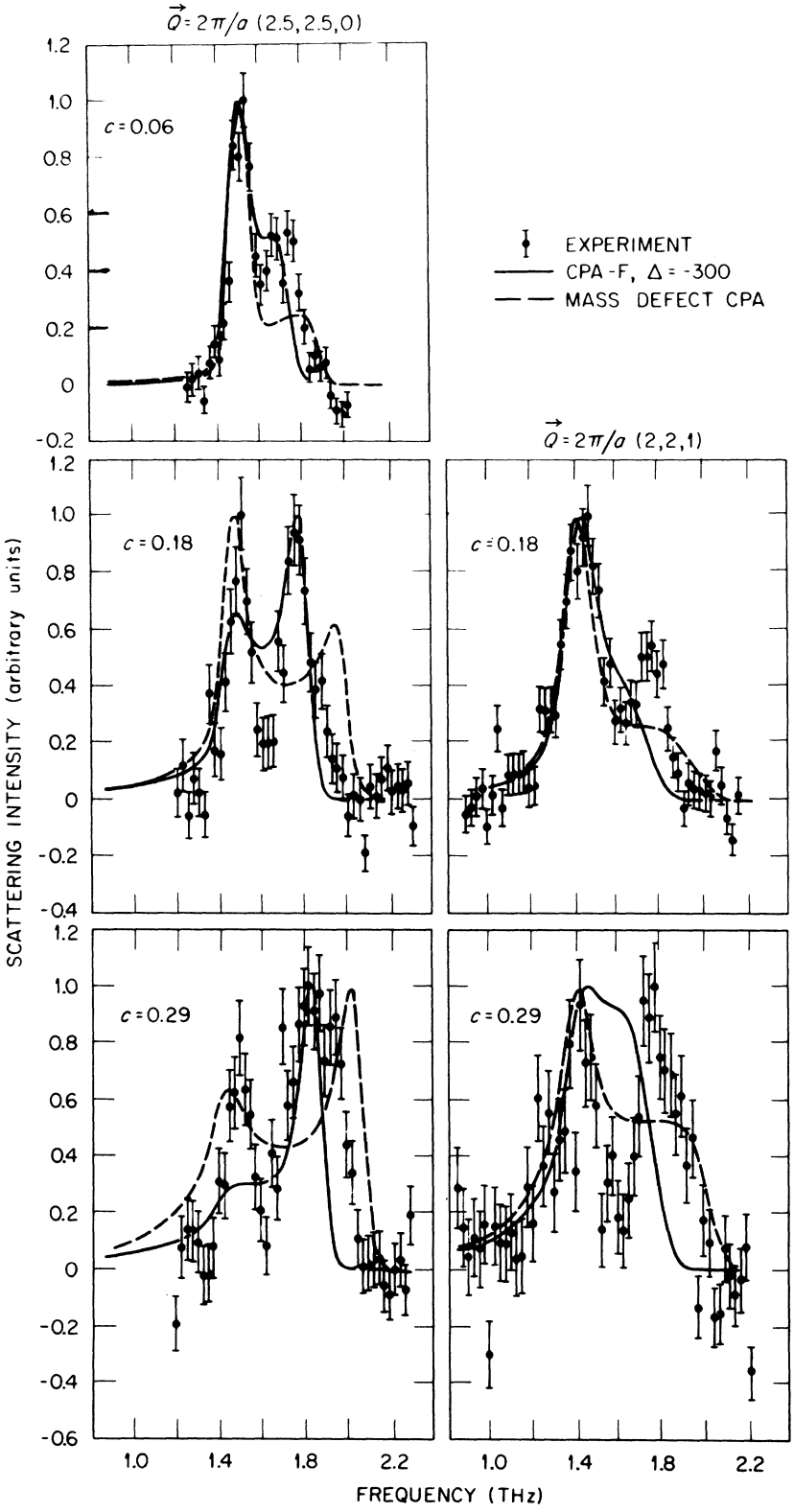

FIG. 5. CPA-F ($\Delta = -300$), mass-defect CPA, and experimental neutron scattering cross sections for two zone boundary modes in $Rb_{1-c}K_c$. Resolution broadening is included in the calculated curves (FWHM = 0.132 THz for $c = 0.18$ and $\vec{Q} = (2\pi/a)(2,2,1)$, FWHM = 0.10 THz otherwise).

For $\vec{Q}=(2\pi/a)(2.5,2.5,0)$, the CPA-F with $\Delta=-300$ is clearly superior to the mass-defect CPA. However, although the CPA-F gives reasonably good values for the peak positions, it does not fit the observed line shapes, which exhibit much sharper structure and extend to higher frequencies. For $\vec{Q}=(2\pi/a)(2,2,1)$, the mass-defect CPA results appear to be better than those of the CPA-F with $\Delta=-300$, but neither is in particularly good agreement with experiment.

To emphasize the difference in line shapes, Fig. 6 compares CPA-F and experimental results for $\vec{Q}=(2\pi/a)(2.40,2.40,0)$ and $c=0.18$, 0.29. In these plots, the measured neutron groups are shown as smooth curves (which were drawn by eye and not by any curve-fitting algorithm). Again, the CPA-F peak positions are close to the experimental values, but the calculated structure is less distinct than that observed.

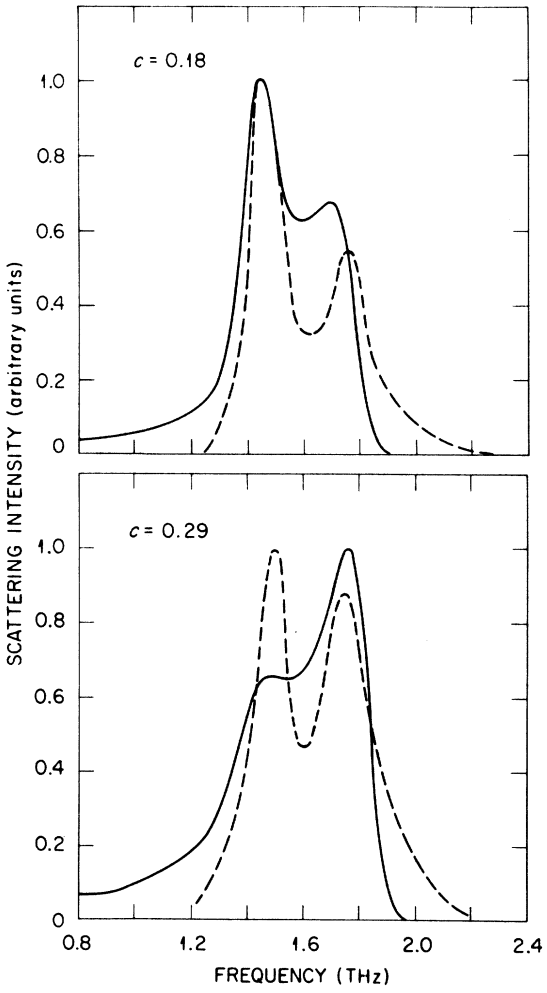

FIG. 6. CPA-F ($\Delta=-300$) and experimental neutron scattering cross sections for $\vec{Q}=(2\pi/a)(2.40,2.40,0)$ and $c=0.18$, 0.29. Instrumental resolution (FWHM = 0.10 THz) has been folded into the calculated curves (full lines), and the experimental results are shown as smooth curves (dashed lines).

The CPA-F with a nearest-neighbor radial force constant change of $\Delta=-300$ appears to give better overall agreement with experiment than the mass-defect CPA. However, it fails to reproduce the measured line shapes for wave vectors near the zone boundary, and it does not give satisfactory results for the concentration and phonon branch dependence of the scattering.

IV. DISCUSSION

There are several possible explanations for the discrepancies between CPA-F and experimental results for $Rb_{1-c}K_c$. Two of these remain wholly within the confines of the model: first, it is possible that volume-dependent effects were not adequately approximated by the use of virtual crystal force constants for the host lattice; second, better agreement with experiment might have been achieved if more than just radial first-neighbor local force constant changes had been included. On the other hand, one of the basic limitations of the CPA-F approach may be the source of the discrepancies. The assumption that the force constants in the alloy superimpose linearly may be a poor approximation. Quite apart from the range and scaling of the local perturbations, the discrepancies may indicate the breakdown of the single-site scattering approach. We believe that this is the most likely explanation, although it cannot be demonstrated conclusively by the failure of a single-site theory which embodies several other approximations. We will briefly discuss each of the explanations offered.

The host crystal force constants, of course, have a strong effect on the in-band peaks in the alloy. They determine not only the unperturbed frequencies, but also, to a considerable extent, the in-band peak shifts and linewidths. In the $E=ct$ theory for mass defects,[6] for example, the in-band shifts and widths are wholly determined by the defect mass and the host crystal density of states. For local modes, however, the primary role of the host crystal force constants is to determine the host crystal bandwidth, and hence the proximity of the local modes to the highest in-band modes. For dilute alloys, at least, the position of the local mode peak is largely established by the defect-host mass difference and force constant changes, while the intrinsic line shape depends on the theory used. For example, if the $E=ct$ approximation gives a δ-function local mode peak at ω_0 in $\langle S(\vec{Q},\omega)\rangle$, then the CPA-F will yield a broadened, typically featureless peak close to ω_0.[31]

With these general considerations in mind, we can argue that the use of virtual crystal host force constants is not an important source of error in the CPA-F calculations. Figure 4 shows that reasonably good agreement is obtained for the in-band peak shifts; in fact, virtual crystal rather than pure Rb force constants were used to improve the CPA-F results for the in-band modes. Figure 5 demonstrates that the local force constant changes determine the positions of the local mode peaks in $\langle S(\vec{Q},\omega)\rangle$, while the calculated line shapes appear to be affected most strongly by the concentration and the separation between local and in-band modes. We also performed CPA-F calculations with modified host crystal force constants based on the mode Grüneisen parameter measurements of Copley *et al.*[38] for Rb, and found neither quantitative improvement in the results nor qualitative changes in the line shapes.

Figure 5 does provide some evidence that better agreement with experiment might be obtained if more force constant changes were included in the CPA-F model. This conclusion is supported by the non-self-consistent theoretical treatments of dilute Cu-Au and Cr-W alloys,[7-9] and by a large body of work on lattice vibrations around isolated defects.[39] With only a radial nearest-neighbor force constant change Δ, fair agreement with the observed peak positions can be obtained with one value ($\Delta \approx -300$) for the [110] longitudinal modes, and another ($\Delta \approx 0$) for the [001] transverse branch. Adding more local force constant changes might make it possible to fit the peak positions for both branches with a single set of values for the parameters. However, as previously noted, incorporating more force constant changes within the CPA-F would increase the computational difficulties of calculations which are already rather complex and time consuming. More importantly, Figs. 5 and 6 show that when relatively good values for the peak positions are obtained in the CPA-F, the structure in the calculated scattering cross sections is considerably less sharp than that observed. The inability of the coherent potential approximation to reproduce sharp structure in the scattering cross section has been noted for at least one other system in which a local mode occurs, namely, $Cu_{0.9}Al_{0.1}$.[19]

More local force constant changes can be handled without great computational difficulty by non-self-consistent single-site theories such as the $E = cI$ approximation,[6-10] the approach of Elliott and Taylor,[11] or the average t-matrix approximation (ATA).[16,21] Ironically, as we have noted, the most obvious unphysical property of these theories is that they produce local mode peaks which are δ functions. It is therefore possible that non-self-consistent calculations might give better agreement with experiment for $Rb_{1-c}K_c$ by producing more sharply structured scattering cross sections in the local mode region. We feel, however, that achieving a better fit in this way, by exploiting a convenient shortcoming of the non-self-consistent theories, would not really explain the data.

Aside from the fact that it is a single-site theory, the most questionable feature of the CPA-F is its assumption that the force constants in the alloy superimpose linearly. This assumption makes it possible to represent the disorder as a sum of functions identified with single sites, the perturbations $\mathfrak{D}^{\gamma(l_i)}$ in Eqs. (2)–(4). Generally, of course, functions of at least pairs as well as single sites are required to describe the alloy. For example, if atoms of types γ and γ' are at sites 0 and n, respectively, then the $0-n$ force constant change cannot generally be expressed as a sum of changes around each of the two sites,

$$\mathfrak{D}^{\gamma(0)\gamma'(n)}(0,n) \neq \mathfrak{D}^{\gamma(0)}(0,n) + \mathfrak{D}^{\gamma'(n)}(0,n). \tag{23}$$

The assumption of linear superposition, by making Eq. (23) an equality rather than an inequality, effectively removes the pair correlations which are present in the Hamiltonian for the general case of off-diagonal disorder.

To our knowledge, no satisfactory self-consistent single-site theory that does not make the assumption of linear superposition has been put forward for phonons. Blackman, Esterling, and Berk[25] (BEB) have proposed an extension of the CPA for the electronic density of states of alloys with off-diagonal as well as diagonal disorder. Shiba[26] has described the limiting case of the BEB approach in which the off-diagonal terms in the Hamiltonian scale geometrically. However, it is not clear that the treatments of BEB or Shiba can be applied to phonons in alloys, because for phonons, translational invariance requires that changes in the force constants between pairs of atoms be accompanied by appropriate changes in the site-diagonal force constants. For electrons in the simple tight-binding models considered, the diagonal term of the Hamiltonian for a particular site depends only on the occupancy of that site; for phonons, the site-diagonal terms depend also on the occupancy of neighboring sites.

If a single-site theory which could handle general force constant changes could be applied to the lattice vibrations of $Rb_{1-c}K_c$, it seems questionable that it would yield detailed agreement with the measured neutron groups. The illustrative electronic densities of states shown by BEB and Shiba for model alloys with off-diagonal disorder exhibit behavior similar to that found in other CPA calculations. The densities of states are smooth and

rather featureless, and no sharp structure occurs in the split-band limit where the defect or "local mode" band splits off from the host band. Also, comparisons of the spectral functions of large clusters with CPA calculations for an electronic system with diagonal disorder[40] show that the CPA fails to reproduce structure present in the spectral functions as well as in the density of states.

Because it is a single-site mean-field theory, the coherent potential approximation does not include true multiple scattering, that is, correlated scattering from pairs, triplets, and larger clusters. As already noted, comparison of CPA and exact results for the density of states[12,27,33,40] show that the CPA gives only a smooth overall picture of an alloy, without the structure arising from cluster-scattering effects. Discrepancies between CPA and exact results are typically most pronounced for local mode bands split-off from the host spectrum.

At the three concentrations at which neutron scattering measurements were done, $c=0.06$, 0.18, and 0.29, the probabilities that at least one defect (K) atom is among the nearest neighbors of a given defect atom are 0.39, 0.80, and 0.94, respectively. The most probable numbers of K neighbors are 0 and 1 for $c=0.06$, 1 and 2 for $c=0.18$, and 2 and 3 for $c=0.29$. Even at the lowest concentration, multisite scattering effects may produce sharper structure in the neutron cross sections than that found in the single-site CPA. We believe that the experimental results for $Rb_{1-c}K_c$, particularly the sharp two-peaked line shapes for wave vectors near the zone boundaries, indicate the need to go beyond the single-site CPA and include cluster scattering effects.

To do this, either analytic approaches or modeling with large clusters can be used. A promising new analytical approach is the augmented space formalism (ASF) originally proposed by Mookerjee[41] and since extended and refined by Kaplan and Gray.[42] The ASF has the proper translational invariance, yields analytic Green's functions, can handle off-diagonal and diagonal disorder, and can be used to treat short-range order as well.

Large cluster calculations are a straightforward way to model alloy properties, and have been used for this purpose for some time.[14,15] Two computationally efficient methods for treating large clusters that have been used recently are the recursion method,[43] which is based on the Lanczos procedure for tridiagonalizing matrices, and the equation of motion method.[33,40] Clusters of thousands of atoms can be handled by these methods without great expenditures of computer time. At present, we are pursuing both the ASF approach and variations of the recursion method for three-dimensional alloy calculations.

ACKNOWLEDGMENTS

We are grateful to W. A. Kamitakahara and J. R. D. Copley for providing the neutron scattering data for $Rb_{1-c}K_c$ alloys. We would also like to thank R. M. Nicklow and R. F. Wood for helpful discussions.

APPENDIX

In very schematic form, we want to outline the procedure used to determine the CPA-F scattering cross section. To make the argument, one additional notational elaboration is required, which is to rewrite Eq. (10) with a superscripted local self-energy as was done for the local perturbations in Eqs. (2)–(4),

$$\underline{E}(l,l';\omega)=\sum_{l_i}\underline{\kappa}^{(l_i)}(l,l';\omega)\,, \tag{A1}$$

$$\underline{\kappa}^{(l_i)}(l,l';\omega)=\sum_{ss'}\underline{K}(s,s';\omega)\delta(l,s+l_i)\delta(l',s'+l_i)\,. \tag{A2}$$

Conditionally averaged Green's functions for the alloy satisfy the following relationships:

$$\langle\underline{G}\rangle=(1-c)\langle\underline{G}^{h(l)}\rangle+c\,\langle\underline{G}^{d(l)}\rangle\,, \tag{A3}$$

$$\langle\underline{G}^{h(l)}\rangle=(1-c)\langle\underline{G}^{h(l)h(l')}\rangle+c\,\langle\underline{G}^{h(l)d(l')}\rangle\,, \tag{A4}$$

$$\langle\underline{G}^{d(l)}\rangle=(1-c)\langle\underline{G}^{d(l)h(l')}\rangle+c\,\langle\underline{G}^{d(l)d(l')}\rangle\,. \tag{A5}$$

Here $\langle\underline{G}^{\gamma(l)}\rangle$ is the configurationally averaged Green's function for the alloy given that there is an atom of type γ at site l, and $\langle\underline{G}^{\gamma(l)\gamma'(l')}\rangle$ is the Green's function when atoms of types γ and γ' are at l and l', respectively. The coherent potential approximation for $\langle\underline{G}\rangle$ is, of course, $\langle\underline{G}\rangle=\underline{G}^0$.

The various conditionally averaged Green's functions in the CPA-F can be found in essentially the same way as they are in mass-defect CPA calculations,[12,44] but with matrix equations spanning the defect space replacing scalar, site-diagonal equations. From Eqs. (1) and (2), we obtain

$$\langle\underline{G}\rangle=\underline{P}+\underline{P}\cdot\left\langle\sum_l\underline{\mathfrak{D}}^{\gamma(l)}\cdot\underline{G}\right\rangle$$

$$=\underline{P}+\underline{P}\cdot\sum_l c_\gamma\underline{\mathfrak{D}}^{\gamma(l)}\cdot\langle\underline{G}^{\gamma(l)}\rangle, \tag{A6}$$

and since $\underline{\mathfrak{D}}^{h(l)}=0$,

$$\langle\underline{G}\rangle=\underline{P}+\underline{P}\cdot\sum_l c\underline{\mathfrak{D}}^{d(l)}\cdot\langle\underline{G}^{d(l)}\rangle. \tag{A7}$$

An alternative expression for $\langle\underline{G}\rangle=\underline{G}^0$ follows from Eqs. (1), (9), and (A1),

$$\langle\underline{G}\rangle=\underline{G}^0=\underline{P}+\underline{P}\cdot\sum_l\kappa^{(l)}\cdot\underline{G}^0. \tag{A8}$$

Comparing Eqs. (A7) and (A8) and equating contri-

butions to $\langle \underline{G} \rangle$ from each site l, we have

$$\langle \underline{G}^{d(l)} \rangle = [c\underline{\mathfrak{D}}^{d(l)}]^{-1} \cdot \underline{\kappa}^{(l)} \cdot \underline{G}^0. \tag{A9}$$

To find $\langle \underline{G}^{d(l)d(l')} \rangle$, we expand Eq. (2) to second order, taking special care with the $l = l'$ contributions,

$$\langle \underline{G} \rangle = \underline{P} + \underline{P} \cdot \sum_l c\underline{\mathfrak{D}}^{d(l)} \cdot \underline{P} + \underline{P} \cdot \sum_l c(1-c)\underline{\mathfrak{D}}^{d(l)} \cdot \langle \underline{G}^{d(l)d(l)} \rangle \cdot \underline{\mathfrak{D}}^{d(l)} \cdot \underline{P} + \underline{P} \cdot \sum_{ll'} c\underline{\mathfrak{D}}^{d(l)} \cdot \langle \underline{G}^{d(l)d(l')} \rangle \cdot c\underline{\mathfrak{D}}^{d(l')} \cdot \underline{P}. \tag{A10}$$

The corresponding expansion of Eq. (10) is

$$\underline{G}^0 = \underline{P} + \underline{P} \cdot \sum_l \underline{\kappa}^{(l)} \cdot \underline{P} + \underline{P} \cdot \sum_{ll'} \underline{\kappa}^{(l)} \cdot \underline{G}^0 \cdot \underline{\kappa}^{(l')} \cdot \underline{P}. \tag{A11}$$

In terms of $\underline{\kappa}^{(l)}$ and $\underline{\mathfrak{D}}^{d(l)}$, Eq. (11) for the local self-energy can be written

$$\underline{\kappa}^{(l)} - c\underline{\mathfrak{D}}^{d(l)} = -\underline{\kappa}^{(l)} \cdot \underline{G}^0 \cdot [\underline{\kappa}^{(l)} - \underline{\mathfrak{D}}^{d(l)}]. \tag{A12}$$

Combining Eqs. (A10)–(A12), we obtain

$$\langle \underline{G}^{d(l)d(l')} \rangle = \delta(l,l')[c\underline{\mathfrak{D}}^{d(l)}]^{-1} \cdot \underline{\kappa}^{(l)} \cdot \underline{G}^0 + [1 - \delta(l,l')][c\underline{\mathfrak{D}}^{d(l)}]^{-1} \cdot \underline{\kappa}^{(l)} \cdot \underline{G}^0 \cdot \underline{\kappa}^{(l')} \cdot [c\underline{\mathfrak{D}}^{d(l')}]^{-1}. \tag{A13}$$

Similar procedures yield the defect-host, host-defect, and host-host Green's functions.

To illustrate the matrix form of the equations for the various conditionally averaged Green's functions, we restore full site notation in Eq. (A13). The result is

$$\begin{aligned} &\langle \underline{G}^{d(l)d(l')}(l+s, l'+s'; \omega) \rangle \\ &\quad = \delta(l,l') \sum_{s_1 s_2'} (c\underline{D})^{-1}(s, s_1) \cdot \underline{K}(s_1, s_1'; \omega) \cdot \underline{G}^0(s_1', s'; \omega) \\ &\quad + [1 - \delta(l,l')] \sum_{s_1 s_1' s_2 s_2'} (c\underline{D})^{-1}(s, s_1) \cdot \underline{K}(s_1, s_1'; \omega) \cdot \underline{G}^0(l + s_1', l' + s_2; \omega) \cdot \underline{K}(s_2, s_2'; \omega) \cdot (c\underline{D})^{-1}(s_2', s'). \end{aligned} \tag{A14}$$

*Research sponsored by ERDA under contract with Union Carbide Corp.

[1] B. Mozer, K. Otnes, and V. W. Myers, Phys. Rev. Lett. 8, 278 (1962).

[2] B. Mozer, K. Otnes, and C. Thaper, Phys. Rev. 152, 535 (1966).

[3] E. C. Svensson, B. N. Brockhouse, and J. M. Rowe, Solid State Commun. 3, 245 (1965); E. C. Svensson and B. N. Brockhouse, Phys. Rev. Lett. 18, 858 (1967).

[4] H. Bjerrum Møller and A. R. Mackintosh, Phys. Rev. Lett. 15, 623 (1965).

[5] R. M. Nicklow, P. R. Vijayaraghavan, H. G. Smith, G. Dolling, and M. K. Wilkinson, in *Neutron Inelastic Scattering* (IAEA, Vienna, 1968), Vol. I, p. 47; R. M. Nicklow, P.R. Vijayaraghavan, H. G. Smith, and M. K. Wilkinson, Phys. Rev. Lett. 20, 1245 (1968).

[6] R. J. Elliott and A. A. Maradudin, in *Inelastic Scattering of Neutrons, Bombay* (IAEA, Vienna, 1965), Vol. I, p. 231.

[7] R. Bruno and D. W. Taylor, Can. J. Phys. 49, 2496 (1971).

[8] K. M. Kesharwani and B. K. Agrawal, Phys. Rev. B 7, 5153 (1973).

[9] K. M. Kesharwani and B. K. Agrawal, Phys. Rev. B 6, 2178 (1972).

[10] K. Lakatos and J. A. Krumhansl, Phys. Rev. 175, 841 (1968); 180, 729 (1969).

[11] R. J. Elliott and D. W. Taylor, Proc. R. Soc. Lond. A 296, 161 (1967).

[12] D. W. Taylor, Phys. Rev. 156, 1017 (1967).

[13] P. Soven, Phys. Rev. 156, 809 (1967).

[14] P. Dean, Proc. R. Soc. Lond. A 260, 263 (1961); Rev. Mod. Phys. 44, 127 (1972).

[15] D. N. Payton, III and W. M. Visscher, Phys. Rev. 154, 802 (1967); 156, 1032 (1967).

[16] P. L. Leath and B. Goodman, Phys. Rev. 181, 1062 (1969).

[17] N. Kunitomi, Y. Tsunoda, and Y. Hirai, Solid State Commun. 13, 495 (1973).

[18] N. Wakabayashi, R. M. Nicklow, and H. G. Smith, Phys. Rev. B 4, 2558 (1971); N. Wakabayashi, *ibid.* 8, 6015 (1973).

[19] T. Kaplan and M. Mostoller, Phys. Rev. B 9, 353 (1974).

[20] W. A. Kamitakahara, Bull. Am. Phys. Soc. 19, 321 (1974); W. A. Kamitakahara and J. R. D. Copley, Solid State Division Annual Progress Report, Oak Ridge National Laboratory Report No. ORNL-4952 (unpublished), 1973, p. 96.

[21] W. A. Kamitakahara and D. W. Taylor, Phys. Rev. B 10, 1190 (1974); W. A. Kamitakahara and B. N.

Brockhouse, *ibid.* 10, 1200 (1974).
[22]M. Mostoller, T. Kaplan, N. Wakabayashi, and R. M. Nicklow, Phys. Rev. B 10, 3144 (1974).
[23]H. G. Smith and N. Wakabayashi, Bull. Am. Phys. Soc. 21, 410 (1976); H. G. Smith, N. Wakabayashi, and M. Mostoller, in *Superconductivity in d- and f-Band Metals (1976)*, edited by D. H. Douglass (Plenum, New York, 1976), p. 223.
[24]P. Soven, Phys. Rev. B 2, 4715 (1970); B. L. Gyorffy, *ibid.* 5, 2382 (1972).
[25]J. A. Blackman, D. M. Esterling, and N. F. Berk, Phys. Rev. B 4, 2412 (1971).
[26]H. Shiba, Prog. Theor. Phys. 46, 77 (1971).
[27]T. Kaplan and M. Mostoller, Phys. Rev. B 9, 1783 (1974).
[28]K. Niizeki, Prog. Theor. Phys. 53, 74 (1975); 54, 1648 (1975).
[29]H. Fukuyama, H. Krakauer, and L. Schwartz, Phys. Rev. B 10, 1173 (1974).
[30]S. Takeno, Prog. Theor. Phys. 40, 942 (1968).
[31]T. Kaplan and M. Mostoller, Phys. Rev. B 10, 3610 (1974).
[32]H. G. Smith, N. Wakabayashi, and R. M. Nicklow, in *Neutron Inelastic Scattering* (IAEA, Vienna, 1972), p. 103.
[33]R. Alben, H. Krakauer, and L. Schwartz, Phys. Rev. B 14, 1510 (1976).
[34]A preliminary account of this work was given in *Proceedings of the Conference on Neutron Scattering*, edited by R. M. Moon (ERDA Report No. CONF-760601-P1, Oak Ridge, Tenn., 1976), Vol. I, p. 202.
[35]R. Benedek and A. Baratoff, Solid State Commun. 13, 385 (1973).
[36]J. R. D. Copley and B. N. Brockhouse, Can. J. Phys. 51, 657 (1973).
[37]R. A. Cowley, A. D. B. Woods, and G. Dolling, Phys. Rev. 150, 487 (1966).
[38]J. R. D. Copley, C. A. Rotter, H. G. Smith, and W. A. Kamitakahara, Phys. Rev. Lett. 33, 365 (1974).
[39]See, for example, R. F. Wood, *Methods in Computational Physics*, edited by B. Alder, S. Fernbach, and M. Rotenberg (Academic, New York, 1976), Vol. 15, p. 119.
[40]R. Alben, M. Blume, H. Krakauer, and L. Schwartz, Phys. Rev. B 12, 4090 (1975).
[41]A. Mookerjee, J. Phys. C 6, 1340 (1973); 6, L205 (1973); A. R. Bishop and A. Mookerjee, *ibid.* C 7, 2165 (1974).
[42]T. Kaplan and L. J. Gray, J. Phys. C 9, L303 (1976); Phys. Rev. B 14, 3462 (1976); J. Phys. C 9, L483 (1976); Phys. Rev. B 15, 3260 (1977).
[43]R. Haydock, V. Heine, and M. J. Kelly, J. Phys. C 5, 2845 (1972); 8, 2591 (1975).
[44]R. J. Elliott, J. A. Krumhansl, and P. L. Leath, Rev. Mod. Phys. 46, 465 (1974).